The influence of IMF clock angle on dayside flux transfer events at Mercury

Roger P. Leyser[1], Suzanne M. Imber[1,2], Steve E. Milan[1], James A. Slavin[2]

[1]Department of Physics and Astronomy, University of Leicester, Leicester, UK
[2]Climate and Space Sciences and Engineering, University of Michigan, Ann Arbor, Michigan, USA

Key Points:

- Large statistical study of dayside FTEs at Mercury
- FTEs at Mercury more prevalent during periods of near-southward IMF
- FTEs form preferentially in the pre-noon sector of Mercury's dayside magnetopause

Corresponding author: Roger Leyser, rpl4@le.ac.uk

Abstract

Analysis of MESSENGER data has shown for the first time that the orientation of the Interplanetary Magnetic Field (IMF) in the magnetosheath of Mercury plays a crucial role in the formation of flux transfer events (FTEs) at the dayside magnetopause. During the first 4 Hermean years of MESSENGER's orbit around Mercury, we have identified 805 FTEs using magnetometer data. Under conditions of near-southward IMF, at least one FTE was detected on nearly 70% of passes through the magnetopause but the observation rate during northward IMF was less than 20%. FTEs were also observed preferentially in the pre-noon sector.

1 Introduction

Mercury was first discovered to have an intrinsic global magnetic field by Mariner 10 [*Ness et al.*, 1974, 1975], and details of the nature of its magnetosphere were refined through measurements made by the MErcury Surface, Space ENvironment, GEochemistry, and Ranging (MESSENGER) spacecraft when it became the first satellite to orbit Mercury [*Anderson et al.*, 2011, 2012]. Mercury's close proximity to the Sun exposes it to the extreme solar wind conditions present at an orbital distance of 0.31-0.47 AU, including an interplanetary magnetic field (IMF) strength of 20-40 nT [*Blomberg et al.*, 2007], $\sim$5 times that measured at Earth, and solar wind number density of 30-70 cm^{-3} [*Blomberg et al.*, 2007], an order of magnitude greater at Mercury [*Baumjohann et al.*, 2006]. Furthermore, the planetary dipole moment at Mercury is about 3 orders of magnitude lower than that at Earth [*Johnson et al.*, 2012; *Johnson and Hauck*, 2016], with a value of 195 nT ${R_M}^3$ [*Anderson et al.*, 2011] (where R_M = 2440 km is the radius of Mercury). The combination of this weak planetary field and the solar wind conditions means the Hermean magnetosphere is extremely small and strongly driven by variable conditions in the solar wind [*Slavin et al.*, 2009]. The mean distance to the magnetopause at the subsolar point is only $1.45R_M$ [*Winslow et al.*, 2013], but during extreme solar wind conditions the magnetopause can be compressed or eroded sufficiently to barely hold the solar wind off the surface, with observations as low as $1.03R_M$ [*Slavin et al.*, 2014].

Magnetic reconnection is an important factor in the interaction between the solar wind and the magnetosphere, eroding the dayside magnetosphere [*Slavin et al.*, 2010a; *Heyner et al.*, 2016] and driving the Dungey cycle of magnetic flux circulation [*Dungey*, 1961; *Imber and Slavin*, 2017], thus allowing entry of solar wind plasma into the magnetosphere [*Raines et al.*, 2015]. At Earth, reconnection on the dayside magnetopause occurs at low latitude primarily when the magnetic shear angle between the planetary field and the IMF in the magnetosheath is high [e.g. *Dungey*, 1961; *Fairfield and Cahill*, 1966; *Perreault and Akasofu*, 1978; *Sonnerup et al.*, 1981]. Antiparallel reconnection at a single X-line connects magnetospheric field lines to draped IMF in the magnetosheath. The newly open field lines are dragged away from the reconnection site by the magnetosheath flow. Helical bundles of open magnetic flux, known as flux transfer events (FTEs) [*Russell and Elphic*, 1978], are commonly observed at the magnetopause of Earth, often with a large azimuthal extent [*Fear et al.*, 2008]. Following the first observation of FTEs at Earth by *Russell and Elphic* [1978], *Lee and Fu* [1985] suggested that the observed bipolar signature in the magnetic field component normal to the magnetopause that is attributed to FTEs could be explained by reconnection occurring at multiple parallel X-lines. This produces a flux rope with its long axis aligned with the X-line, and connected magnetically to both the IMF and the planetary magnetic field.

FTEs have been observed at Earth at all locations on the magnetopause under a wide range of solar wind conditions by single spacecraft such as International Sun-Earth Explorer 1 (ISEE-1) [*Kawano and Russell*, 1996, 1997] and Interball-1 [e.g. *Sibeck et al.*, 2005; *Korotova et al.*, 2012], in addition to many multi-spacecraft missions, including Cluster [e.g. *Fear et al.*, 2008], Time History of Events and Macroscale Interactions during Substorms (THEMIS) [e.g. *Korotova et al.*, 2011; *Trenchi et al.*, 2016], and most recently Magnetospheric Multiscale (MMS) [e.g. *Eastwood et al.*, 2012; *Farrugia et al.*, 2016; *Hasegawa et al.*, 2016], allowing for accurate determination of the orientation and scale size of the FTEs. Such detailed measurements are not possible with the single MESSENGER spacecraft, however observations have nonetheless not only confirmed the presence of FTEs at Mercury, but also shown them to be ubiquitous in nature [*Slavin et al.*, 2009, 2010b,a, 2012; *Imber et al.*, 2014]. Indeed, studies by *Slavin et al.* [2012] and *Imber et al.* [2014] have demonstrated that FTEs at Mercury occur more frequently than those seen at Earth, and are considerably larger with respect to the size of the magnetosphere. This is attributed to the reconnection-driven formation of FTEs being greatly enhanced due to the stronger interaction between the IMF and the Hermean magnetic field.

One way of quantifying the reconnection rate is to calculate the ratio of inflow velocity at a reconnection site to the Alfvén velocity of the outflow [*Sonnerup*, 1974]. This dimensionless reconnection rate can also be expressed as a ratio of the component of the magnetic field normal to the boundary to the total field just inside the magnetopause [*Sonnerup et al.*, 1981]. At Earth, reported values vary considerably, ranging from as little as 0.01 [*Fuselier et al.*, 2005] to ∼0.1 [*Sonnerup et al.*, 1981]. Many of these values were obtained from case studies of individual magnetopause crossings, however, and in the largest statistical study to date *Mozer and Retinò* [2007] analysed 22 events and determined an average reconnection rate of 0.046. At Mercury, only one study has investigated this quantity at the dayside magnetopause. *DiBraccio et al.* [2013] used measurements of the magnetic field for 43 magnetopause crossings, and calculated a mean dimensionless reconnection rate of 0.15, validating the theory of stronger interactions between the planetary field and the IMF at Mercury [*Slavin and Holzer*, 1979]. However, *DiBraccio et al.* [2013] found that the dimensionless reconnection rate displayed very little dependence on the magnetic shear angle between the two regimes, contrary to similar investigations at Earth [e.g. *Sonnerup*, 1974]. They attributed this to a low Alfvén Mach number, M_A, and low plasma β (the ratio of thermal pressure to magnetic pressure) in the Hermean magnetosheath. Under these conditions, a large plasma depletion layer forms due to the pile-up of magnetic flux in the magnetosheath [*Gershman et al.*, 2013], leading to enhanced reconnection rates and enabling reconnection over a wider range of shear angles than observed at the Earth.

In this paper we present a large statistical study of FTEs observed near the dayside magnetopause using data obtained by MESSENGER's Magnetometer [*Anderson et al.*, 2007] during the first four Hermean years after orbital insertion. Our analysis suggests that the formation of FTEs at Mercury exhibits a strong dependence on the orientation of the IMF, with a considerably enhanced production rate for magnetopause crossings during which the magnetic shear angle was large.

2 Observations

On 18 March 2011, MESSENGER orbital insertion placed the spacecraft into an eccentric, high-inclination orbit about Mercury with a period of 12 h. The orbital plane was fixed in inertial space such that the periapsis precessed completely around the planet once every Hermean year (88 days). In this study, we have used data obtained by the Magnetometer onboard MESSENGER, which at full resolution provided 20 samples/s [*Anderson et al.*, 2007], during the interval spanning orbital insertion until 9 March 2012. By including exactly 4 Hermean years, we have ensured approximately even coverage of all magnetic local time (MLT) sectors over the duration of this study, with the exception of 19 orbits between 24 May and 2 June 2011, when the Magnetometer collected no data near the dayside magnetopause traversals. These orbits are symmetric about 12 h MLT and confined to a small MLT range, however, so no dawn-dusk bias is introduced by the lack of data in this period. Furthermore, the number of missing passes is small compared to the total number of passes in the affected MLT sectors, so no biases have been introduced. Data are presented in the Mercury solar magnetospheric (MSM) coordinate system, in which the X axis points towards the Sun, the origin is centered on the internal dipole of Mercury and the Z axis is aligned with magnetic north. This coordinate system is then rotated to account for Mercury's changing orbital motion with respect to an average solar wind velocity of 400 $km\ s^{-1}$, producing the resultant aberrated MSM coordinate system (MSM′).

Our focus in this study is the dayside magnetosphere, therefore the magnetic field data have been examined for every encounter of MESSENGER with the magnetopause sunward of X′ = -0.5 R_M. An example of a MESSENGER orbit is shown in Figures 1(e-f), with model locations for the bow shock and magnetopause, as given by *Winslow et al.* [2013], and the components of the magnetic field measured by the MESSENGER magnetometer are shown in panels (a-d). Panels (g-l) show a subsection of these data, spanning the inbound crossings of the bow shock and magnetopause on this orbit. Several large amplitude FTEs are present in the data, as indicated by the arrows in Figure 1j.

2.1 Identifying magnetopause crossings and flux transfer events

Every spacecraft pass through the dayside magnetopause during the time interval considered was visually inspected for individual magnetopause crossings and FTE signatures in the magnetic field data. A pass here refers to a traversal of the magnetopause region, during which multiple individual magnetopause crossings may be observed. The magnetopause crossings were identified by a sudden large change in the magnetic field strength or, for cases when the magnitude varied only slightly, by a rotation in the magnetic field vector. In both scenarios, the identification of crossings was aided by a significant reduction in the amplitude and frequency of fluctuations in the magnetic field on the magnetospheric side of the magnetopause. Flux transfer events were initially identified on the basis of a clear increase in the total field strength compared to the background level, accompanied by a bipolar signature in one or more field components. Throughout the period considered here, in 727 passes during which the magnetopause was traversed sunward of X′ = -0.5 R_M, we identified a total of 1717 individual magnetopause crossings and 805 FTEs for which the above conditions were satisfied. In the 306 passes on which these FTEs were observed, 818 individual magnetopause crossings were identified, yielding an average observation rate of 0.98 FTEs per magnetopause crossing on passes containing FTEs.

3 Analysis

3.1 Magnetopause and FTE locations

The location of each of the 1717 magnetopause crossings identified in this work is projected into the MSM $X' - Y'$ and $X' - Z'$ planes in Figures 2a and 2b. Due to the highly elliptical polar orbit of the MESSENGER spacecraft, the inbound portion of the orbit through the dayside magnetosphere often passes through the northern magnetic cusp. The spacecraft therefore regularly skims the magnetopause at high northern latitudes, resulting in multiple detectable magnetopause crossings on a single orbit. Additionally, ongoing reconnection or variable solar wind conditions can result in a magnetopause that repeatedly moves back and forth over the spacecraft, again leading to the observation of multiple crossings on a single pass.

Figure 2a shows that crossings were observed approximately equally in all MLT sectors in the dayside magnetosphere, and that on average the magnetopause crossings occurred near to the location given by the *Winslow et al.* [2013] model for the majority of orbits considered here. There appears to be a substantial spread in the distance of the observed crossings from the model location, which is likely due to crossings occurring during a range of Hermean seasons, resulting in significant changes to the compression of the magnetosphere by the solar wind between aphelion and perihelion [*Zhong et al.*, 2015]. The location of the FTEs identified in this study are presented in panels (c) and (d) as red circles, with the magnetopause crossings indicated in grey for context. It can be seen that the majority of FTEs were observed near local noon, and the approximately equal data coverage in MLT means this is manifested as a greater percentage observation of FTEs within 3 h MLT of local noon.

Figures 2b and 2d show two distinct latitudinal groupings of both magnetopause crossings and FTEs, which can be attributed to orbital bias. The group near the subsolar point have been observed during MESSENGER's "hot season" orbits, when periapsis was on the dayside and the spacecraft passed outwards through the dayside magnetopause at low latitude. Half a Hermean year later, the orbital trajectory of MESSENGER carries it into the magnetosphere at high latitude, close to the northern cusp, producing the higher latitude group of magnetopause crossings and FTEs.

In a previous study of a smaller number of events over a different time period, *Imber et al.* [2014] observed a larger number of FTEs in the dawn sector than the dusk, a bias that is also present in these data. This is more apparent in Figure 3a, which shows that the largest number of FTEs are seen at a magnetic local time of 10 h, with 288 FTEs observed between 9-11 h MLT compared to 238 between 13-15 h MLT. This asymmetry may be due to the unusual conditions observed in the IMF during the period examined [*James et al.*, 2017; *Lockwood et al.*, 2017], whereby in the majority of passes IMF B_X is positive, leading to a similar bias towards $-B_Y$ due to the Parker spiral [*Parker*, 1958]. This in turn leads to increased probability of near-antiparallel fields in the pre-noon sector of the portion of the magnetosphere sampled by MESSENGER.

3.2 Influence of IMF clock angle on FTE formation

Many studies have investigated the parameters influencing dayside reconnection rates at Earth [e.g. *Akasofu*, 1981; *Mozer and Retinò*, 2007; *Milan et al.*, 2007, 2012; *Newell et al.*, 2007], however there has only been one such study at Mercury. *DiBraccio et al.* [2013] analysed the magnetic field data from 43 magnetopause crossings to determine a dimensionless reconnection rate, and concluded that for their dataset there was no significant variation with magnetic shear angle. The FTEs observed in this study were formed by reconnection on the dayside magnetopause, and have an average duration of 3.27s, calculated by recording the start and end time of the bipolar signature of each event. This is similar to the $\sim$2-3 s durations observed by *Imber et al.* [2014] and *Slavin et al.* [2012]. Given the high velocities of these structures observed at Earth, and the small spatial scale of the Hermean magnetosphere, it is reasonable to assume that the IMF direction had not changed significantly from the time of formation of the FTEs to their observation. In this study, we analyse the dependence of FTE observation on IMF orientation.

The orientation of the magnetosheath field was recorded over 1 minute just outside the outermost magnetopause crossing on each orbit to give a measurement of the clock angle in the magnetosheath, where 0° is directed northwards and +90° is directed towards $+B_{Y'}$ and the total number of FTEs in each 30° bin has been plotted in Figure 3b. In agreement with studies at equivalent locations in the Earth's magnetosphere [*Kawano and Russell*, 1997; *Sibeck et al.*, 2005, e.g.], this shows a clear general trend towards greater FTE occurrence during intervals of near-southward IMF, and therefore nearly anti-parallel fields, although any potential statistical bias introduced by multiple FTEs in a single pass or an uneven distribution of observed IMF orientations needs to be accounted for.

A histogram of the occurrence frequency of the magnetosheath clock angle for every pass on which at least 1 FTE was observed is presented in Figure 4a. Multiple FTEs observed on a single crossing are therefore grouped into a single event, resulting in a similar distribution to that presented in Figure 3 with some asymmetries removed. FTEs were observed on 306 of the 727 total passes inspected, during which 818 magnetopause crossings were detected, and Figure 4b shows the distribution of clock angles observed across all magnetopause encounters. The approximately equal coverage of all clock angle orientations indicates that variations in observation rates cannot be attributed to sampling bias. By dividing the values in Figure 4a by those in Figure 4b we obtain the percentage occurrence of at least 1 FTE for each clock angle, as indicated in Figure 4c. For clock angles close to zero, indicating a magnetosheath magnetic field pointing approximately along the positive $B_{Z'}$ axis, FTEs have been detected on fewer than 20% of passes, whereas for near-southward IMF the observation rate increases to nearly 70%. During periods of northward IMF, the reconnection X-line is expected to exist tailward of the cusp regions, therefore we would not expect to observe any FTEs generated at low latitudes near the dayside magnetopause. However, MESSENGER's orbit samples significant portions of the high latitude magnetosphere, so we would still expect to observe FTEs that have formed under northward IMF if reconnection is taking place in these locations.

Out of a total of 727 passes, events exhibiting the required magnetic field signature were observed on 306, although many crossings contained multiple events. Considering how ubiquitous FTEs have been found to be at Mercury in previous studies [*Slavin et al.*, 2012; *Imber et al.*, 2014], this ratio is perhaps lower than expected. However, the formation of FTEs at the dayside magnetopause has been shown for the first time to be significantly less likely during northward IMF, and these orientations contribute a substantial portion of the data examined here. Therefore, the higher ratios seen in previous studies could be explained by an IMF orientation during those periods that is more favourable for FTE formation. Furthermore, in requiring a clear increase in the core field component, we have restricted our sample to those events for which MESSENGER entered the flux rope directly. As a result, many events exhibiting similar features have not been included, such as the travelling compression regions identified by *Slavin et al.* [2012].

In addition to the effect of the IMF clock angle on the observation rate of FTEs in the Hermean magnetosphere, the events in this study were also found to exhibit a small dependence on the strength of the magnetosheath field. In general, a stronger magnetosheath field resulted in the observation of more FTEs per pass, reaching a maximum at $\sim$140 nT, above which there were too few occurrences for results to be statistically significant. However, this increase is only small, resulting in a trend that is considerably less significant than the clock angle effects presented here.

There are several reasons why the results presented here contrast so strongly with those observed by *DiBraccio et al.* [2013]. First of all, although the formation of FTEs requires reconnection, the reconnection rate itself is not measured here, so it is difficult to directly compare the results. Secondly, the sample size used by *DiBraccio et al.* [2013] was considerably smaller than that utilised here. The large dataset investigated over a long time interval in this study is likely to have averaged out the effects of other parameters, thereby producing a more accurate reflection of how the IMF orientation alone influences the observation rate of FTEs at Mercury. Furthermore, the analysis performed by *DiBraccio et al.* [2013] utilised only crossings with a well defined normal direction to the magnetopause, as determined from minimum variance analysis of the magnetic field data. The presence of FTEs during a crossing may result in a poorly defined magnetopause normal, therefore crossings containing FTEs may have been excluded from their analysis, possibly leading to a calculation of the reconnection rate only under conditions less favourable to FTE formation.

4 Conclusions

727 passes of magnetic field data taken by the MESSENGER spacecraft were visually inspected for flux transfer event signatures near the dayside magnetopause encounters. Observation of FTEs is shown to be strongly dependent on the orientation of the IMF in the magnetosheath. FTEs with clear signatures were identified in 306 of the 727 passes through the magnetopause sunward of MSM $X' = -0.5\ R_M$, with a total of 805 FTEs observed. During periods of near-southward IMF at least 1 FTE was observed on nearly 70% of passes, whereas during northward IMF the observation rate is less than 20%.

The spatial distribution of the identified FTEs peaks at a magnetic local time of 10 h, and more FTEs were observed throughout the pre-noon sector than post-noon, corroborating the results of *Imber et al.* [2014]. Additionally, the identified magnetopause crossings agree well with the *Winslow et al.* [2013] model for large parts of the dayside magnetosphere. Some crossings on the dawn and dusk flanks are seen closer to Mercury than predicted, but these occurred during perihelion, when stronger solar wind forcing produced a more compressed magnetosphere.

The upcoming BepiColombo mission will provide the opportunity to expand further on the analysis performed herein, due to improved instruments including a magnetometer with even greater temporal resolution than the MESSENGER magnetometer [*Glassmeier et al.*, 2010] and additional plasma measurements [*Saito et al.*, 2010]. Additionally, the orbital paths will provide considerably greater magnetopause coverage, allowing for the observation of FTEs across a much larger range of latitudes, including for the first time significant coverage of the dayside magnetopause in the southern hemisphere.

Figure 1. Magnetic field data in MSM′ coordinates for a complete MESSENGER orbit. Panels (a)-(d) show $B_{X'}$, $B_{Y'}$, $B_{Z'}$ and $|B|$ respectively. The spacecraft trajectory during the course of this orbit is projected onto the (e) Y'-X' and (f) Z'-X' planes. Model locations of the bow shock (blue) and magnetopause (green), as given by the *Winslow et al.* [2013] models, are also shown. Panels (g)-(l) show the same as (a)-(f) above, but for a shorter interval spanning the inbound bow shock and magnetopause crossings with some FTE signatures visible, as indicated by the arrows.

Figure 2. Locations of the magnetopause crossings in this study, projected onto the (a) MSM $X' - Y'$ and (b) MSM $X' - Z'$ planes. The locations of the identified FTEs are shown in the same projections in panels (c) and (d), with the magnetopause crossings also indicated in grey for comparison. The model magnetopause location predicted by *Winslow et al.* [2013] is indicated by the dashed line.

Figure 3. Histograms showing (a) the locations of the observed FTEs in MLT and (b) how the total number of FTEs observed varies with the clock angle of the IMF in the magnetosheath. The total number of FTEs, n, is also indicated.

Figure 4. Histograms showing (a) the number of passes during each IMF orientation for which at least 1 FTE was observed, (b) the occurrence of each clock angle, and (c) percentage of magnetopause crossings under each IMF orientation during which at least 1 FTE was observed. The number of passes with at least 1 FTE, n, is also indicated.

Acknowledgments

R.P.L. was supported by a Science and Technology Facilities Council (STFC) studentship. S.M.I. was supported by The Leverhulme Trust and STFC grant ST/K001000/1. S.E.M was supported by STFC grant ST/N000749/1. J.A.S was supported by NASA's Heliophysics Supporting Research (NNX15AJ68G) and Living With a Star (NNX16AJ67G) programs. The MESSENGER data used in this study are available from the Planetary Data System (PDS): http://pds.jpl.nasa.gov. The event list is available on request.

References

Akasofu, S.-I. (1981), Energy coupling between the solar wind and the magnetosphere, *Space Sci. Rev.*, *28*(2), 121–190, doi:10.1007/BF00218810.

Anderson, B. J., M. H. Acuña, D. A. Lohr, J. Scheifele, A. Raval, H. Korth, and J. A. Slavin (2007), The Magnetometer Instrument on MESSENGER, *Space Science Reviews*, *131*(1), 417–450, doi:10.1007/s11214-007-9246-7.

Anderson, B. J., C. L. Johnson, H. Korth, M. E. Purucker, R. M. Winslow, J. A. Slavin, S. C. Solomon, R. L. McNutt, J. M. Raines, and T. H. Zurbuchen (2011), The global magnetic field of Mercury from MESSENGER orbital observations., *Science (New York, N.Y.)*, *333*(6051), 1859–62, doi:10.1126/science.1211001.

Anderson, B. J., C. L. Johnson, H. Korth, R. M. Winslow, J. E. Borovsky, M. E. Purucker, J. A. Slavin, S. C. Solomon, M. T. Zuber, and R. L. McNutt (2012), Low-degree structure in Mercury's planetary magnetic field, *Journal of Geophysical Research: Planets*, *117*(E12), doi:10.1029/2012JE004159.

Baumjohann, W., A. Matsuoka, K. Glassmeier, C. Russell, T. Nagai, M. Hoshino, T. Nakagawa, A. Balogh, J. Slavin, R. Nakamura, and W. Magnes (2006), The magnetosphere of mercury and its solar wind environment: Open issues and scientific questions, *Advances in Space Research*, *38*(4), 604 – 609, doi: http://dx.doi.org/10.1016/j.asr.2005.05.117, mercury, Mars and Saturn.

Blomberg, L. G., J. A. Cumnock, K.-H. Glassmeier, and R. A. Treumann (2007), Plasma Waves in the Hermean Magnetosphere, *Space Sci. Rev.*, *132*(2-4), 575–591, doi: 10.1007/s11214-007-9282-3.

DiBraccio, G. A., J. A. Slavin, S. A. Boardsen, B. J. Anderson, H. Korth, T. H. Zurbuchen, J. M. Raines, D. N. Baker, R. L. McNutt, and S. C. Solomon (2013), MESSENGER observations of magnetopause structure and dynamics at Mercury, *Journal of Geophysical Research: Space Physics*, *118*(3), 997–1008, doi:10.1002/jgra.50123.

Dungey, J. W. (1961), Interplanetary Magnetic Field and the Auroral Zones, *Phys. Rev. Lett.*, *6*, 47–48, doi:10.1103/PhysRevLett.6.47.

Eastwood, J. P., T. D. Phan, R. C. Fear, D. G. Sibeck, V. Angelopoulos, M. Ieroset, and M. A. Shay (2012), Survival of flux transfer event (FTE) flux ropes far along the tail magnetopause, *J. Geophys. Res. Sp. Phys.*, *117*(8), doi:10.1029/2012JA017722.

Fairfield, D. H., and L. J. Cahill (1966), Transition region magnetic field and polar magnetic disturbances, *J. Geophys. Res.*, *71*(1), 155–169, doi:10.1029/JZ071i001p00155.

Farrugia, C. J., B. Lavraud, R. B. Torbert, M. Argall, I. Kacem, W. Yu, L. Alm, J. Burch, C. T. Russell, J. Shuster, J. Dorelli, J. P. Eastwood, R. E. Ergun, S. Fuselier, D. Gershman, B. L. Giles, Y. V. Khotyaintsev, P. A. Lindqvist, H. Matsui, G. T. Marklund, T. D. Phan, K. Paulson, C. Pollock, and R. J. Strangeway (2016), Magnetospheric Multiscale Mission observations and non-force free modeling of a flux transfer event immersed in a super-Alfvénic flow, *Geophys. Res. Lett.*, *43*(12), 6070–6077, doi: 10.1002/2016GL068758.

Fear, R. C., S. E. Milan, A. N. Fazakerley, E. A. Lucek, S. W. H. Cowley, and I. Dandouras (2008), The azimuthal extent of three flux transfer events, *Annales Geophysicae*, *26*(8), 2353–2369, doi:10.5194/angeo-26-2353-2008.

Fuselier, S. A., K. J. Trattner, S. M. Petrinec, C. J. Owen, and H. Réme (2005), Computing the reconnection rate at the Earth's magnetopause using two spacecraft observations, *J. Geophys. Res. Sp. Phys.*, *110*(A6), A06,212, doi:10.1029/2004JA010805.

Gershman, D. J., J. A. Slavin, J. M. Raines, T. H. Zurbuchen, B. J. Anderson, H. Korth, D. N. Baker, and S. C. Solomon (2013), Magnetic flux pileup and plasma depletion in Mercury's subsolar magnetosheath, *J. Geophys. Res. (sp. Physics)*, *118*, 7181–7199, doi:10.1002/2013JA019244.

Glassmeier, K. H., H. U. Auster, D. Heyner, K. Okrafka, C. Carr, G. Berghofer, B. J. Anderson, A. Balogh, W. Baumjohann, P. Cargill, U. Christensen, M. Delva, M. Dougherty, K. H. Fornaçon, T. S. Horbury, E. A. Lucek, W. Magnes, M. Mandea, A. Matsuoka, M. Matsushima, U. Motschmann, R. Nakamura, Y. Narita, H. O'Brien, I. Richter, K. Schwingenschuh, H. Shibuya, J. A. Slavin, C. Sotin, B. Stoll, H. Tsunakawa, S. Vennerstrom, J. Vogt, and T. Zhang (2010), The fluxgate magnetometer of the BepiColombo Mercury Planetary Orbiter, *Planet. Space Sci.*, *58*(1-2), 287–299, doi:10.1016/j.pss.2008.06.018.

Hasegawa, H., N. Kitamura, Y. Saito, T. Nagai, I. Shinohara, S. Yokota, C. J. Pollock, B. L. Giles, J. C. Dorelli, D. J. Gershman, L. A. Avanov, S. Kreisler, W. R. Paterson, M. O. Chandler, V. Coffey, J. L. Burch, R. B. Torbert, T. E. Moore, C. T. Russell, R. J. Strangeway, G. Le, M. Oka, T. D. Phan, B. Lavraud, S. Zenitani, and M. Hesse (2016), Decay of mesoscale flux transfer events during quasi-continuous spatially-extended reconnection at the magnetopause, *Geophys. Res. Lett.*, doi:10.1002/2016GL069225.

Heyner, D., C. Nabert, E. Liebert, and K.-H. Glassmeier (2016), Concerning reconnection-induction balance at the magnetopause of Mercury, *J. Geophys. Res. Sp. Phys.*, *121*(4), 2935–2961, doi:10.1002/2015JA021484.

Imber, S. M., and J. A. Slavin (2017), MESSENGER Observations of Magnetotail Loading and Unloading: Implications for Substorms at Mercury, *J. Geophys. Res. Sp. Phys.*, doi:10.1002/2017JA024332.

Imber, S. M., J. A. Slavin, S. A. Boardsen, B. J. Anderson, H. Korth, R. L. McNutt, and S. C. Solomon (2014), MESSENGER observations of large dayside flux transfer events: Do they drive Mercury's substorm cycle?, *Journal of Geophysical Research: Space Physics*, *119*(7), 5613–5623, doi:10.1002/2014JA019884, 2014JA019884.

James, M. K., S. M. Imber, E. J. Bunce, T. K. Yeoman, M. Lockwood, M. J. Owens, and J. A. Slavin (2017), Interplanetary magnetic field properties and variability near Mercury's orbit, *J. Geophys. Res. Sp. Phys.*, doi:10.1002/2017JA024435.

Johnson, C. L., and S. A. Hauck (2016), A whole new Mercury: MESSENGER reveals a dynamic planet at the last frontier of the inner solar system, *J. Geophys. Res. Planets*, doi:10.1002/2016JE005150.

Johnson, C. L., M. E. Purucker, H. Korth, B. J. Anderson, R. M. Winslow, M. M. H. Al Asad, J. A. Slavin, I. I. Alexeev, R. J. Phillips, M. T. Zuber, and S. C. Solomon (2012), MESSENGER observations of Mercury's magnetic field structure, *Journal of Geophysical Research: Planets*, *117*(E12), doi:10.1029/2012JE004217.

Kawano, H., and C. T. Russell (1996), Survey of flux transfer events observed with the ISEE 1 spacecraft: Rotational polarity and the source region, *J. Geophys. Res. Sp. Phys.*, *101*(A12), 27,299–27,308, doi:10.1029/96JA02703.

Kawano, H., and C. T. Russell (1997), Survey of flux transfer events observed with the ISEE 1 spacecraft: Dependence on the interplanetary magnetic field, *J. Geophys. Res. Sp. Phys.*, *102*(A6), 11,307–11,313, doi:10.1029/97JA00481.

Korotova, G. I., D. G. Sibeck, A. Weatherwax, V. Angelopoulos, and V. Styazhkin (2011), THEMIS observations of a transient event at the magnetopause, *J. Geophys. Res. Sp. Phys.*, *116*(7), 1–13, doi:10.1029/2011JA016606.

Korotova, G. I., D. G. Sibeck, and V. I. Petrov (2012), Interball-1 observations of flux transfer events, *Ann. Geophys.*, *30*(10), 1451–1462, doi:10.5194/angeo-30-1451-2012.

Lee, L. C., and Z. F. Fu (1985), A theory of magnetic flux transfer at the Earth's magnetopause, *Geophys. Res. Lett.*, *12*(2), 105–108, doi:10.1029/GL012i002p00105.

Lockwood, M., M. J. Owens, S. M. Imber, M. K. James, E. J. Bunce, and T. K. Yeoman (2017), Coronal and heliospheric magnetic flux circulation and its relation to open solar flux evolution, *J. Geophys. Res. Sp. Phys.*, *122*(6), 5870–5894, doi:10.1002/2016JA023644.

Milan, S. E., G. Provan, and B. Hubert (2007), Magnetic flux transport in the Dungey cycle: A survey of dayside and nightside reconnection rates, *J. Geophys. Res. Sp. Phys.*, *112*(1), doi:10.1029/2006JA011642.

Milan, S. E., J. S. Gosling, and B. Hubert (2012), Relationship between interplanetary parameters and the magnetopause reconnection rate quantified from observations of the expanding polar cap, *J. Geophys. Res. Sp. Phys.*, *117*(3), doi:10.1029/2011JA017082.

Mozer, F. S., and A. Retinò (2007), Quantitative estimates of magnetic field reconnection properties from electric and magnetic field measurements, *J. Geophys. Res.*, *112*(A10), A10,206, doi:10.1029/2007JA012406.

Ness, N. F., K. W. Behannon, R. P. Lepping, Y. C. Whang, and K. H. Schatten (1974), Magnetic field observations near Mercury: Preliminary results from Mariner 10, *Science (New York, N.Y.)*, *185*(4146), 151–160, doi:10.1126/science.185.4146.151.

Ness, N. F., K. W. Behannon, R. P. Lepping, and Y. C. Whang (1975), The magnetic field of Mercury, 1, *Journal of Geophysical Research*, *80*(19), 2708–2716, doi: 10.1029/JA082i019p02828.

Newell, P. T., T. Sotirelis, K. Liou, C.-I. Meng, and F. J. Rich (2007), A nearly universal solar wind-magnetosphere coupling function inferred from 10 magnetospheric state variables, *J. Geophys. Res. Sp. Phys.*, *112*(A1), doi:10.1029/2006JA012015.

Parker, E. N. (1958), Dynamics of the Interplanetary Gas and Magnetic Fields., *Astrophys. J.*, *128*, 664, doi:10.1086/146579.

Perreault, P., and S.-I. Akasofu (1978), A study of geomagnetic storms, *Geophys. J. R. Astron. Soc.*, *54*(3), 547–573, doi:10.1111/j.1365-246X.1978.tb05494.x.

Raines, J. M., G. A. DiBraccio, T. A. Cassidy, D. C. Delcourt, M. Fujimoto, X. Jia, V. Mangano, A. Milillo, M. Sarantos, J. A. Slavin, and P. Wurz (2015), Plasma Sources in Planetary Magnetospheres: Mercury, doi:10.1007/s11214-015-0193-4.

Russell, C. T., and R. C. Elphic (1978), Initial ISEE magnetometer results - Magnetopause observations, *Space Science Reviews*, *22*, 681–715, doi:10.1007/BF00212619.

Saito, Y., J. Sauvaud, M. Hirahara, S. Barabash, D. Delcourt, T. Takashima, and K. Asamura (2010), Scientific objectives and instrumentation of Mercury Plasma Particle Experiment (MPPE) onboard MMO, *Planet. Space Sci.*, *58*(1-2), 182–200, doi:10.1016/j.pss.2008.06.003.

Sibeck, D. G., G. I. Korotova, V. Petrov, V. Styazhkin, and T. J. Rosenberg (2005), Flux transfer events on the high-latitude magnetopause: Interball-1 observations, *Ann. Geophys.*, *23*(11), 3549–3559, doi:10.5194/angeo-23-3549-2005.

Slavin, J. A., and R. E. Holzer (1979), The effect of erosion on the solar wind stand-off distance at Mercury, *J. Geophys. Res.*, *84*(A5), 2076, doi:10.1029/JA084iA05p02076.

Slavin, J. A., M. H. Acuña, B. J. Anderson, D. N. Baker, M. Benna, S. A. Boardsen, G. Gloeckler, R. E. Gold, G. C. Ho, H. Korth, S. M. Krimigis, R. L. McNutt, J. M. Raines, M. Sarantos, D. Schriver, S. C. Solomon, P. Trávníček, and T. H. Zurbuchen (2009), MESSENGER Observations of Magnetic Reconnection in Mercury's Magnetosphere, *Science*, *324*(5927), 606–610, doi:10.1126/science.1172011.

Slavin, J. A., B. J. Anderson, D. N. Baker, M. Benna, S. A. Boardsen, G. Gloeckler, R. E. Gold, G. C. Ho, H. Korth, S. M. Krimigis, R. L. McNutt, L. R. Nittler, J. M. Raines, M. Sarantos, D. Schriver, S. C. Solomon, R. D. Starr, P. M. Trávnícek, and T. H. Zurbuchen (2010a), MESSENGER observations of extreme loading and unloading of Mercury's magnetic tail., *Science*, *329*(5992), 665–8, doi:10.1126/science.1188067.

Slavin, J. A., R. P. Lepping, C.-C. Wu, B. J. Anderson, D. N. Baker, M. Benna, S. A. Boardsen, R. M. Killen, H. Korth, S. M. Krimigis, W. E. McClintock, R. L. McNutt, M. Sarantos, D. Schriver, S. C. Solomon, P. Trávnícek, and T. H. Zurbuchen (2010b), MESSENGER observations of large flux transfer events at Mercury, *Geophysical Research Letters*, *37*(2), doi:10.1029/2009GL041485, l02105.

Slavin, J. A., S. M. Imber, S. A. Boardsen, G. A. DiBraccio, T. Sundberg, M. Sarantos, T. Nieves-Chinchilla, A. Szabo, B. J. Anderson, H. Korth, T. H. Zurbuchen, J. M. Raines, C. L. Johnson, R. M. Winslow, R. M. Killen, R. L. McNutt, and S. C. Solomon (2012), MESSENGER observations of a flux-transfer-event shower at Mercury, *Journal of Geophysical Research: Space Physics*, *117*(A12), doi:10.1029/2012JA017926, a00M06.

Slavin, J. A., G. A. DiBraccio, D. J. Gershman, S. M. Imber, G. K. Poh, J. M. Raines, T. H. Zurbuchen, X. Jia, D. N. Baker, K.-H. Glassmeier, S. A. Livi, S. A. Boardsen, T. A. Cassidy, M. Sarantos, T. Sundberg, A. Masters, C. L. Johnson, R. M. Winslow, B. J. Anderson, H. Korth, R. L. McNutt, and S. C. Solomon (2014), MESSENGER observations of Mercury's dayside magnetosphere under extreme solar wind conditions, *Journal of Geophysical Research: Space Physics*, *119*(10), 8087–8116, doi:

10.1002/2014JA020319, 2014JA020319.
Sonnerup, B. U. Ö. (1974), Magnetopause reconnection rate, *J. Geophys. Res.*, *79*(1), 1546–1549, doi:10.1029/JA079i010p01546.
Sonnerup, B. U. Ö., G. Paschmann, I. Papamastorakis, N. Sckopke, G. Haerendel, S. J. Bame, J. R. Asbridge, J. T. Gosling, and C. T. Russell (1981), Evidence for magnetic field reconnection at the Earth's magnetopause, *J. Geophys. Res. Sp. Phys.*, *86*(A12), 10,049–10,067, doi:10.1029/JA086iA12p10049.
Trenchi, L., R. C. Fear, K. J. Trattner, B. Mihaljcic, and A. N. Fazakerley (2016), A sequence of flux transfer events potentially generated by different generation mechanisms, *J. Geophys. Res. A Sp. Phys.*, *121*(9), 8624–8639, doi:10.1002/2016JA022847.
Winslow, R. M., B. J. Anderson, C. L. Johnson, J. A. Slavin, H. Korth, M. E. Purucker, D. N. Baker, and S. C. Solomon (2013), Mercury's magnetopause and bow shock from MESSENGER Magnetometer observations, *Journal of Geophysical Research: Space Physics*, *118*(5), 2213–2227, doi:10.1002/jgra.50237.
Zhong, J., W. X. Wan, Y. Wei, J. A. Slavin, J. M. Raines, Z. J. Rong, L. H. Chai, and X. H. Han (2015), Compressibility of Mercury's dayside magnetosphere, *Geophys. Res. Lett.*, *42*(23), 10,135–10,139, doi:10.1002/2015GL067063.

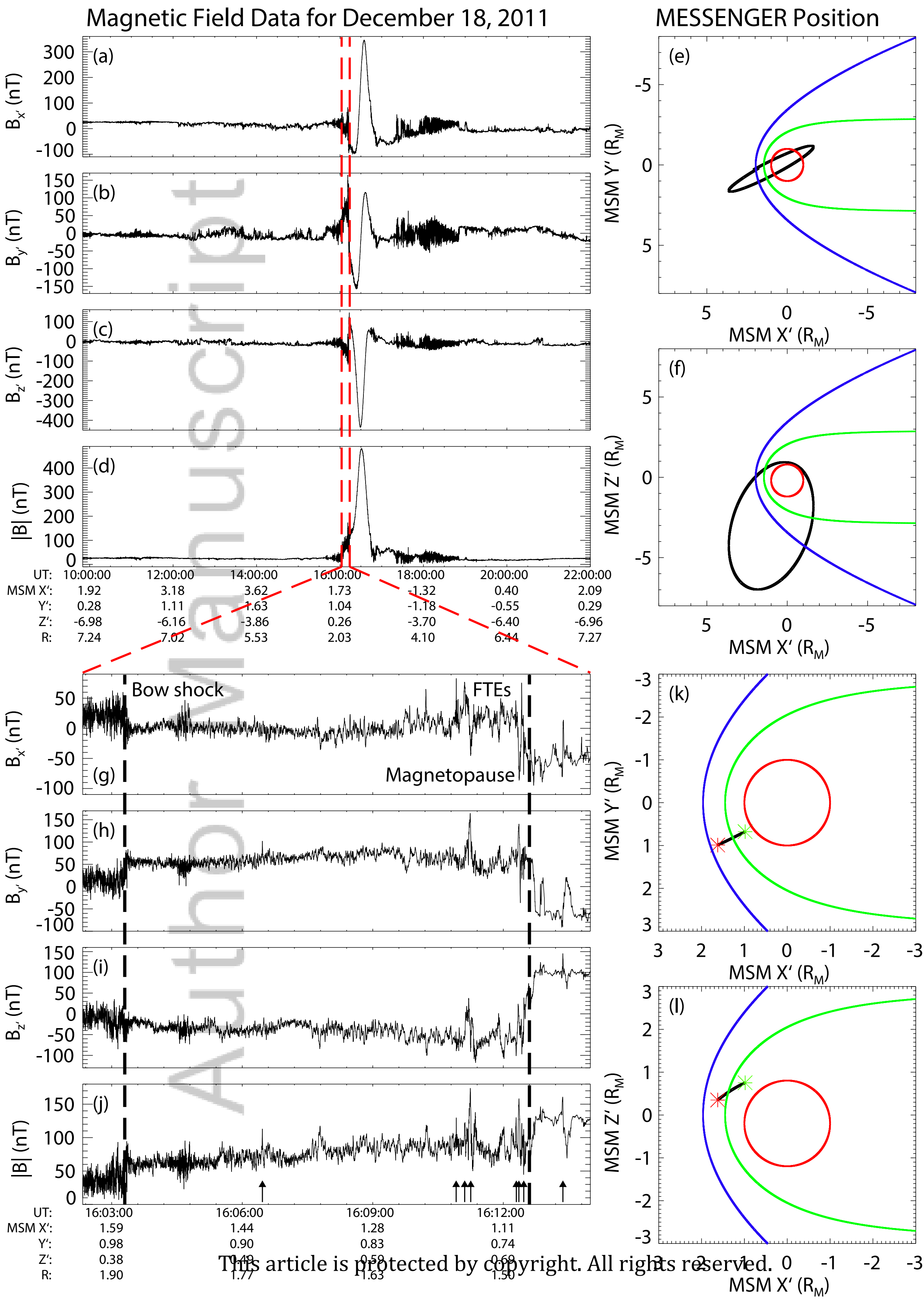
Magnetic Field Data for December 18, 2011
MESSENGER Position
(a)
B_x' (nT)
(b)
B_y' (nT)
(c)
B_z' (nT)
(d)
|B| (nT)
UT: 10:00:00 12:00:00 14:00:00 16:00:00 18:00:00 20:00:00 22:00:00
MSM X': 1.92 3.18 3.62 1.73 -1.32 0.40 2.09
Y': 0.28 1.11 1.63 1.04 -1.18 -0.55 0.29
Z': -6.98 -6.16 -3.86 0.26 -3.70 -6.40 -6.96
R: 7.24 7.02 5.53 2.03 4.10 6.44 7.27
(e)
MSM Y' (R_M)
MSM X' (R_M)
(f)
MSM Z' (R_M)
MSM X' (R_M)
Bow shock
FTEs
Magnetopause
(g)
B_x' (nT)
(h)
B_y' (nT)
(i)
B_z' (nT)
(j)
|B| (nT)
UT: 16:03:00 16:06:00 16:09:00 16:12:00
MSM X': 1.59 1.44 1.28 1.11
Y': 0.98 0.90 0.83 0.74
Z': 0.38
R: 1.90 1.77 1.63 1.50
(k)
MSM Y' (R_M)
MSM X' (R_M)
(l)
MSM Z' (R_M)
MSM X' (R_M)

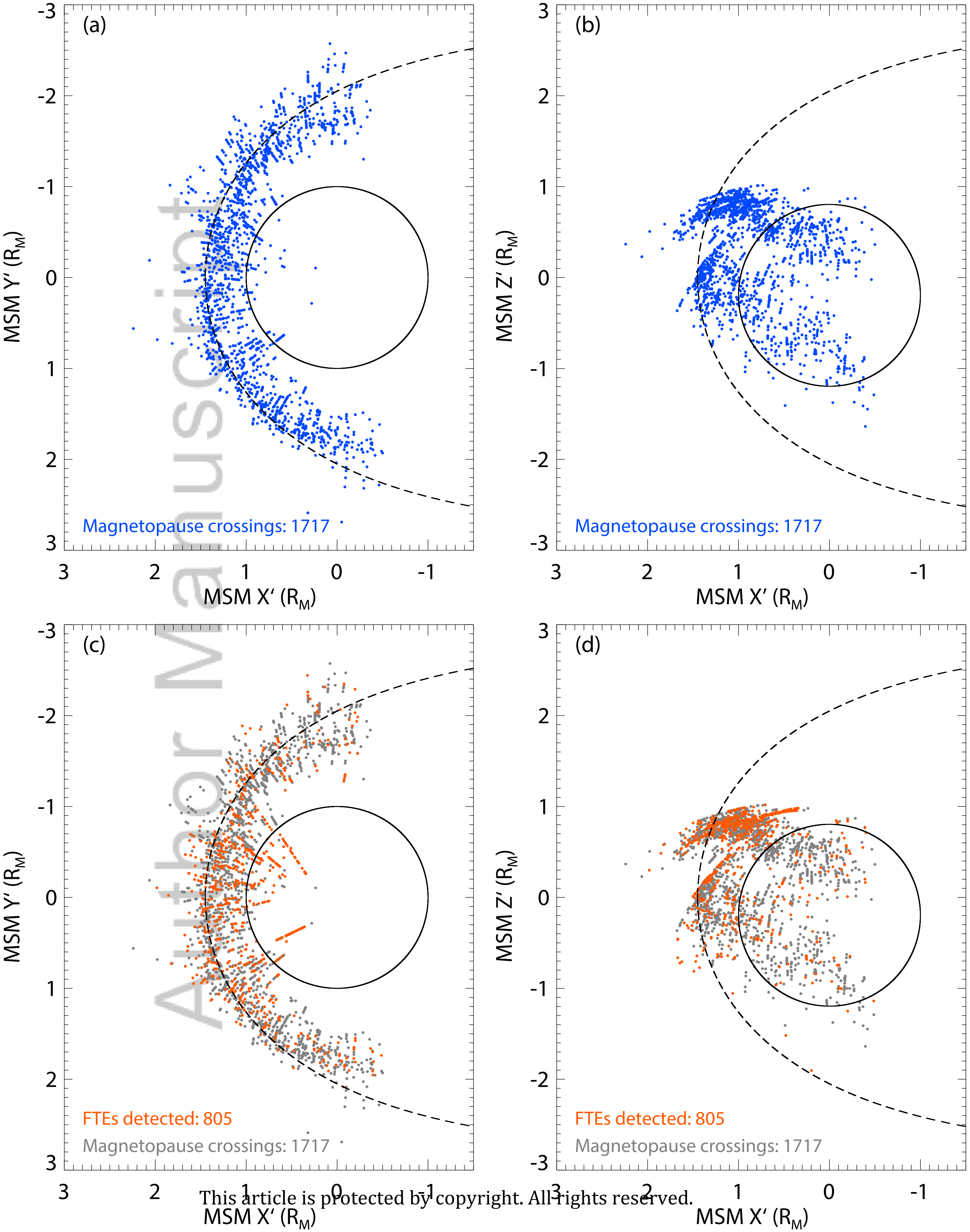
(a)
(b)
(c)
(d)
MSM Y′ (R_M)
MSM Z′ (R_M)
MSM X′ (R_M)
Magnetopause crossings: 1717
FTEs detected: 805
Author Manuscript

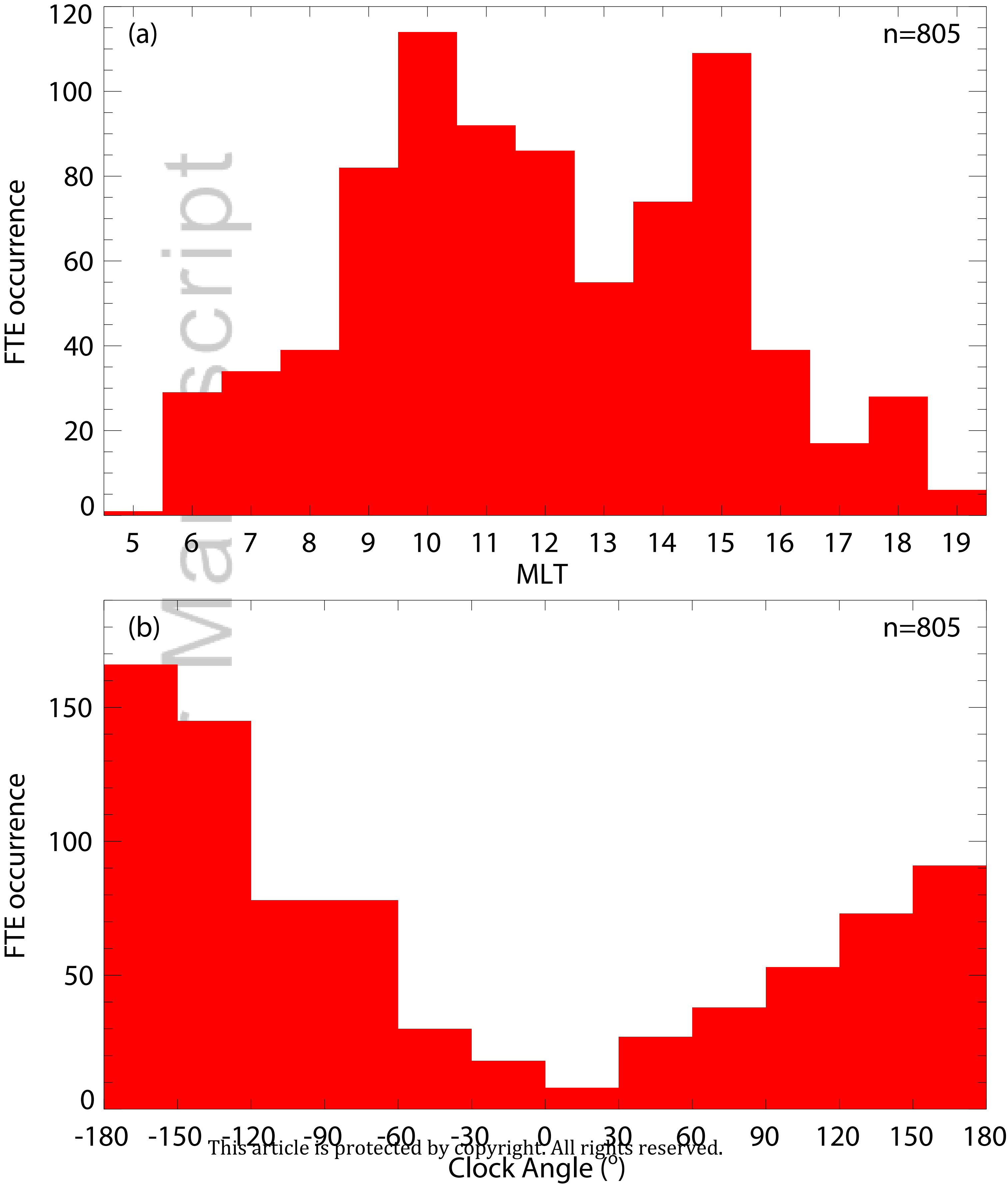
(a)
n=805
FTE occurrence
0
20
40
60
80
100
120
5
6
7
8
9
10
11
12
13
14
15
16
17
18
19
MLT
(b)
n=805
FTE occurrence
0
50
100
150
-180
-150
-120
-90
-60
-30
0
30
60
90
120
150
180
Clock Angle (°)

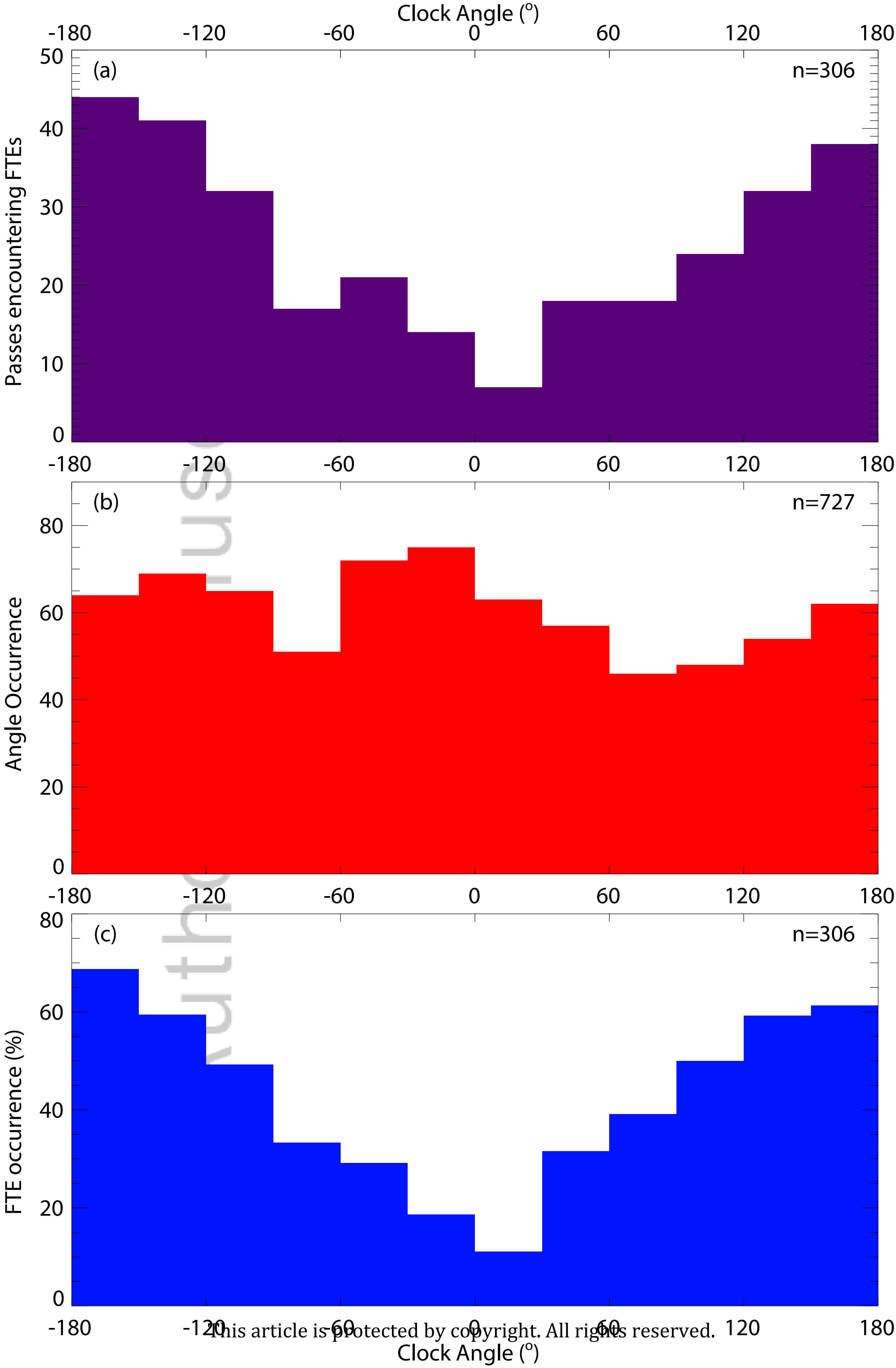
Clock Angle (°)
-180
-120
-60
0
60
120
180
50
40
30
20
10
0
(a)
n=306
Passes encountering FTEs
80
60
40
20
0
(b)
n=727
Angle Occurrence
80
60
40
20
0
(c)
n=306
FTE occurrence (%)
Clock Angle (°)